Transmission Geometry Laser Lighting with a Compact Emitter

Caroline E Reilly, Guillaume Lheureux, Clayton Cozzan, Emet Zeitz, Tal S Margalith, Shuji Nakamura, Ram Seshadri, Claude Weisbuch, Steven P Denbaars

Title

Transmission Geometry Laser Lighting with a Compact Emitter

Journal

physica status solidi (a), 217(22)

ISSN

1862-6300 1862-6319

Authors

Reilly, Caroline E
Lheureux, Guillaume
Cozzan, Clayton
et al.

Publication Date

2020-09-30

DOI

10.1002/pssa.202000391

Peer reviewed

Transmission geometry laser lighting with a compact emitter

Caroline E. Reilly, Guillaume Lheureux, Clayton Cozzan, Emet Zeitz, Tal Margalith, Shuji Nakamura, Ram Seshadri, Claude Weisbuch, and Steven P. DenBaars*

C. E. Reilly, Dr. G. Lheureux, Dr. C. Cozzan, E. Zeitz, Dr. T. Margalith, Prof. S. Nakamura, Prof. R. Seshadri, Prof. C. Weisbuch, Prof. S. P. DenBaars
University of California, Santa Barbara, California 93106, USA
E-mail: cereilly@ucsb.edu

Prof. C. Weisbuch
Laboratoire de Physique de la Matière Condensée, CNRS-Ecole Polytechnique, IP Paris, 91128 Palaiseau Cedex, France

Keywords: Solid-state lighting, laser lighting, nitrides, single crystal phosphors

Laser lighting systems can take many form factors for applications such as spotlighting, general illumination, or decorative lighting. The use of lasers in conjunction with phosphors for white lighting leads to questions about incorporating the various package elements. Some practical considerations of a transmission geometry system implementing a blue laser and a yellow Ce:YAG single crystal phosphor are discussed, with specific focus on color tuning and the optical efficiency of the single crystal. A compact emitter is demonstrated with examples of modifications to increase the system performance and complexity. Moving from a cool white system to a warm white system has been done through the addition of a red light such as a red laser or red phosphor. The single crystal phosphor component needs to allow light to be coupled in from the laser and have high extraction efficiency. A wavelength-selective reflective coating has been implemented to address these concerns, which increased the luminous efficacy of the system. Engineering the phosphor

element using this concept may allow for single crystal phosphors to be viable options for future laser lighting systems.

1. Introduction

1.1. Solid-state lighting

Innovations in lighting technology have often focused on increased efficiency and decreased cost as the primary benchmarks for accepting new lighting platforms into everyday use. The invention of the blue LED and the rise of solid-state lighting has led to enormous energy savings along with decreased costs for lighting. The United States annual energy savings from LED adoption increased from $675 million in 2012 to $4.7 billion in 2016, with LEDs accounting for only 12.6% of lighting installations in 2016 [1,2]. This trend continues to increase, with LEDs making up an estimated 19% of lighting installations in 2017 and an expected 84% of lighting installations by 2035 [3]. LEDs have also brought about a substantial change in how we use lights. Solid-state lighting has the benefit of being much smaller and brighter than previous lighting platforms, enabling new form factors and applications [4,5]. Along with LEDs successfully replacing conventional fixtures such as standard lightbulbs, more decorative or futuristic applications have been made possible with solid-state lighting. From car logos that light up to wearable displays for augmented reality to the indicator light on video game controllers, LEDs have permeated every aspect of modern life.

Laser lighting has been a topic of increasing interest for several years, with the idea being to use a laser diode as the electrically driven solid-state light source. Whereas LEDs struggle with decreased efficiencies

under high power operation [6], lasers can efficiently output high optical powers. In the case of white lighting applications, a blue laser can pump a yellow phosphor such that the blue and yellow mix together to output white light. Other color phosphors can be used as a replacement for or in conjunction with the yellow phosphor to tune the color point and temperature. For example, with a blue source and a standard Ce:YAG yellow phosphor, only a cool white color temperature above 4000K can be achieved, with warmer color temperatures achievable with the addition of a red source such as a red phosphor [7,8]. In addition to different colors of phosphors being useful, different morphologies of phosphors – including single crystals, powders, and ceramics – can be incorporated into laser lighting designs [9–12].

In this work, a framing introduction will be presented in section 1 which provides background to the current state of the field. Section 1.2 serves to contextualize the area of laser lighting within solid-state lighting, explaining why one may wish to use lasers over LEDs. In section 1.3, a concise overview of solid-state lighting metrics is presented. Section 1.4 then provides the reasoning for the emitter design choices of a single crystal phosphor and transmission geometry. Section 1.5 provides an overview discussion of heating effects in laser lighting systems.

1.2. The benefit of lasers

One inherent difference between LEDs and lasers is the radiant power at peak wall-plug efficiency (WPE). LEDs tend to have the highest efficiency at current densities under 10 A/cm^2, whereas lasers peak at current densities on the order of 10000 A/cm^2. For good efficiency, high

power fixtures, an array of LEDs is necessary to achieve the radiant power of a single laser. Although the peak WPE of record blue lasers, ~45% [13], is significantly less than that of blue LEDs, there are application specific advantages of using lasers over LEDs. The difference in emitting area, around 10 mm^2 for LEDs and 0.1 mm^2 for lasers, has financial and technological implications. By shrinking the emitting area from that of an LED system to that of a laser system, less area is necessary in terms of epitaxial growth and phosphor materials. This has the potential to reduce the costs of laser-based white lighting systems as the technology matures. In terms of technological advancements, shrinking the emitting area provides a benefit to the étendue of the system.

Étendue describes the areal and angular spread of a light source and is a property of the light emitter that cannot be decreased without introducing losses into the system. For any light source, a small solid angle may be achieved by blocking light emitted at higher solid angles, resulting in loss of efficiency and brightness. Therefore, a source with a small étendue should be chosen for directional lighting applications such as spotlights, decorative/museum lighting, and headlights. Some high brightness, directional applications are not well served by LED sources which do not produce enough radiant power over a small enough angle – their étendue is too large. In an LED system, the étendue limiting factor is the die size of the LED, where increasing light power while maintaining efficiency involves increasing the die size because of droop at higher current densities. By shrinking down the emitting area to that of a laser-based system, an emitter closer to that of a point source can be achieved,

which can then be directed by lossless or low-loss optics onto a small light down-converter such as a phosphor. The phosphor used in a white laser lighting system then becomes the étendue limiting element and must be as small as possible while considering other constraints such as conversion under high optical power density. Improvements in high brightness, directional applications replace LED platforms with laser based ones [14–16], for example in car headlights [17].

Laser lighting can further supplement the current LED lighting platforms by opening up applications and allowing exploration of new form factors for lighting. In the area of visible light communication (VLC), lasers win over LEDs by having a higher modulation speed, allowing for faster data transmission [18–20]. The unique ability of lasers to efficiently couple into optical fibers allows the heat-generating, sensitive electro-optic components to be located far away from the illuminated area and for the laser light to travel efficiently over long distances. Applications such as horticulture may find this remote-source lighting useful, where the light is delivered to the plant without exposing the light-emitting component to heat and humidity [21]. It may also be possible to leverage leaky fibers, in which the coupled laser light is leaked along the length of the fiber to provide light over a large area [22,23]. In this design, the light could be transmitted as blue laser light through the length of the fiber and then converted to white light with a phosphor material integrated in or attached to the leaky fiber. Underwater lighting could become less bulky, as the laser coupled into the fiber would not have to be waterproofed. The

capability to separate the emission area and the electrical components widely opens the design space for laser-based lighting.

1.3. Metrics: Efficiency, efficacy, and color

For laser lighting to become relevant in a given use case, it needs to match or exceed what can be done with LEDs in terms of achieving high efficiency performance and high-quality white light while maintaining low cost. Phosphor converted laser lighting systems have many similarities to white LED systems based on blue LEDs and yellow phosphors. The same terminology and metrics apply to white laser lighting as those used for white LED lighting. An important metric for both systems is luminous efficacy, which is a measure of the optical power output of the system for a given electrical power input, its efficiency, weighted by the human eye response function. Efficacy is expressed in lumens per watt, whereas efficiency is reported in percentages and does not consider the perceived luminosity. For lighting applications, efficacy is a key concept and can be estimated in the blue laser-yellow phosphor system by Equation 1, where WPE is the wall plug efficiency of the laser [24,25], OE is optical efficiency, QY is the quantum yield of the phosphor, SS is the Stokes shift of the blue to yellow conversion [8,26,27], and LER is the luminous efficacy of radiation.

$$Efficacy\left(\frac{lm}{W}\right)=WPE\,x\,OE\,x\,QY\,x\,SS\,x\,LER\left(\frac{lm}{W}\right)$$

(1)

The efficacy of any white laser lighting emitter – here defined as the laser, phosphor, and package together without any focusing optical

components – is impacted by metrics of all three components. Improvements in epitaxial material quality, growth schemes, and process development continue to push the WPE of blue lasers towards theoretical values. Commercial blue laser diodes packaged in TO9 cans were utilized herein, where the WPE may be measured directly by comparing the input electrical energy to the output optical energy of the packaged laser. For systems discussed in this work, OE can be separated into several categories, including extraction efficiency, in-coupling, and package efficiency. Extraction efficiency refers to the light successfully escaping the phosphor and in-coupling is the laser light that does not get reflected at the initial phosphor surface. Extraction efficiency and in-coupling are both largely dictated by the phosphor plate design. Package efficiency encompasses losses due to other package or optical components and can vary widely based on choices in package geometry, design, and materials. While this work focuses on the emitter, the OE of a complete lighting system also includes the luminaire, such that for a perfectly efficient luminaire, any light coming from the emitter is used productively as illumination. A visualization of energy flow through the emitter is given in **Figure 1**.

The phosphor conversion process affects the emitter efficiency and can be separated into two factors: the QY of the phosphor and the SS of the conversion. Equation 1 is considered an estimation rather than an exact calculation due to the simplification made that all the light in the system undergoes the QY and SS effects. This is not the case, as these factors relate to the phosphor conversion and some blue light is not converted.

The QY, also known as quantum efficiency, is the percentage of photons absorbed by the phosphor that are reemitted at a longer wavelength [8,10]. This accounts for absorbed photons but not photons that pass through the phosphor without undergoing absorption. Phosphor converting materials have been a target of considerable research efforts and have reached high QY values of above 95% [28]. The SS is another factor of the phosphor, given as the percentage of absorbed photon energy that is reemitted in a longer wavelength photon. The SS is based off the energies of the absorbed and emitted photons and some degree of SS is unavoidable as a fundamental loss in blue-to-yellow conversion when using phosphors.

While efficacy is connected to the color of the light, color is a separately defined metric typically given in terms of x and y color coordinates corresponding to a defined CIE color diagram [29,30]. By varying the amount of yellow phosphor in the system, the ratio of yellow light to blue light can be altered which in turn changes the color of the output light. In addition to color coordinates, metrics of correlated color temperature (CCT) and color rendering index (CRI) are useful when discussing white lighting for illumination [5,27]. CCT defines the ‘warmness’ or ‘coolness’ of a white light source in terms of black body radiation, therefore it is in units of kelvin where values around 5000K correspond to ‘cool’ or blue-ish white light and values around 2700 K correspond to ‘warm’ or more red-ish white light [31,32]. Reaching a warm white light is considered critical for the adoption of laser lighting. CRI describes how well an illumination source shows the ideal color of objects, defined by a series of standards,

with 100 being a perfect CRI [33,34]. Although color is a separate measurement system than efficacy, there is a relationship between the two metrics due to the varying sensitivity of the human eye to different wavelengths of light. The maximum value of efficacy for a given emission spectrum is given in units of lumens per watt and is known as LER [16,35]. LER is a measure of the luminous optical power of a system per the radiant power and has different values for different spectra. Multiplying the LER of a system by the efficiency, in terms of a percentage or optical watts per electrical watts, gives the luminous efficacy.

1.4. Design choices: Single crystals and transmission

With many form factors imaginable, and more yet unimagined, varied optical geometries and converting materials need to be explored to allow for the largest possible design space for laser lighting. For white lighting applications utilizing a blue laser and a yellow phosphor converting material, two main geometries exist for the conversion process – transmission and reflection. Figure 2 depicts the idealized geometries. In transmission geometry, the laser light passes through a converting phosphor and some of the blue laser light comes through on the other side, such that white light is produced on the side of the phosphor opposite the laser. Transmission geometry is similar to how white, phosphor-converted LEDs function. In reflection geometry, a laser is directed towards a phosphor with some of the light converted to yellow light and some of the laser light undergoing specular reflection and scattering. This geometry takes advantage of the directionality of the laser light but is not possible for LEDs without some optical element in between.

Both transmission and reflection geometries need to be explored in order to provide laser lighting fixture designers with the greatest number of possibilities and considerations for any given application.

Single crystal phosphors in a transmission geometry will be the focus of this work. Single crystal phosphors have been used as the converting material for LEDs [36]. However, single crystals are more expensive than other phosphor morphologies and are therefore not cost effective for LEDs with an omnidirectional emission over a relatively large area. Additionally, coupling the light from the LED into the single crystal is inefficient without further optics. Laser emission has a much smaller beam size than that of LED emission and the directionality of lasers allows better coupling into the single crystal phosphor. As the phosphor plate used could be relatively small in a laser lighting design, single crystals could provide a cost-effective option to replace the silicone encapsulated phosphor of white light LED systems.

This work focused on a simplified transmission geometry laser lighting design for white lighting applications which utilized a blue laser and a single crystal yellow phosphor as the fundamental components. Cost-saving and design-simplifying methods were adopted. No lenses were utilized to focus the laser and the emitter was not encompassed within a luminaire. The creation of a luminaire in order to improve uniformity and further manage the device emission remains an open question for this geometry and was not explored in the present work as there would be a strong interaction between the envisioned luminaire geometry and the emitter design. This compact setup comprised of a TO9 commercial blue

laser, a copper heat sink, and a machined copper phosphor holder with prongs to mount a single crystal Ce:YAG phosphor plate for testing. The phosphor plate plus the compact setup together comprised the compact emitter. Shown in Figure 3, the compact emitter was the approximate size of a standard lightbulb when fitted with a simple reflector. Although not the focus of this work, heating effects can be detrimental to the operation of laser lighting devices, therefore contact between the single crystal phosphor and the prongs of the holder was key, in addition to contact between the phosphor holder and the laser heat sink. Simulations and experimental testing have been conducted on phosphor plate design and optical elements, with experimental details in section 4.

1.5. Heating effects

In the earlier days of white LED solid-state lighting, heating effects were a concern in terms of lowering device performances over time [37–39]. While this has largely been solved for LEDs, lasers have a significantly higher power density and lower efficiency, both of which contribute to more concerns with heating. For any laser lighting system, heat management is a challenge that needs to be overcome for widespread adoption. Heating effects in white laser lighting can be separated into laser device heating and phosphor heating. Under high power operation, lasers produce a significant amount of heat that needs to be dissipated to prevent degradation of the device. Self-heating in lasers can lead to thermal rollover and eventual device failure. For this reason, proper external heat sinking for the laser is a concern for any laser-based lighting

system to ensure the stability of the laser. Operating the laser in a pulsed mode rather than under continuous wave operation may ultimately be another way to reduce these effects. In this work, the copper heat sink in which the TO-9 can laser diode was mounted served to help with extracting the heat away from the laser under operation. This heat sink was machined in-house rather than being commercially purchased due to the need to mount the phosphor as close as possible to the output of the TO-9 can. It was noted that under long-term continuous operation a secondary external heat sink was also necessary.

For white lighting at high powers, heating of the phosphor is also a concern. Phosphor heating stems largely from Stokes shift heating due to the energetic down-conversion of light, given the very high phosphor quantum efficiency. The energy difference between the incoming and outgoing light is lost as heat. A quantum yield less than unity will also contribute to heat generation, as will any absorption from encapsulant materials used. For lower-powered devices such as LEDs, this effect has been found to be manageable, however for high-powered lasers the amount of heat generated scales significantly. Standard silicone encapsulants used in white LEDs provide insufficient thermal management for laser lighting purposes [11,40]. Single crystal phosphors have been shown to have high quantum efficiency which is not quenched until high temperatures [41]. Ceramic or single crystal phosphors with low Ce doping fare much better due to their higher thermal conductivity and high thermal quenching resistance [10,42–45]. In the case of the most heavily used yellow phosphor, Ce:YAG, the solubility limits of Ce permit only very

low concentrations in single crystals, thereby increasing quenching resistance compared to more highly doped systems typical for powders in silicone [46]. Single-crystal Ce:YAG phosphors with relatively low Ce-doping (0.2% to 0.3%) were the focus of this work.

To reduce the concern of reaching high phosphor temperatures, heat sinking of the phosphor remains an important consideration. Depending on the geometry of the system, this can be particularly challenging. For a reflection geometry, a phosphor may be mounted directly on a heat sink that allows for extraction of heat away from the phosphor [11]. In a transmission geometry, heat sinking through contacting the phosphor involves the use of materials with high thermal conductivity and high transparency or reflectivity. The single crystal may be mounted on or held between two sheets of material or mounted through minimized contact with another package component such as a reflective metal. For this work, the single crystal was mounted in a copper holder to allow for enough heat sinking to show proof of concept designs. The contact between the phosphor and the copper holder was critical to extract the heat away from the phosphor. Additionally, the copper phosphor holder was to be in contact with the laser heat sink in order to provide further thermal management.

2. Discussion

In section 2.1, the color point was tuned by varying the thickness of the phosphor plate. The implementation of a red laser (section 2.2) or a red phosphor (section 2.3) for the purpose of obtaining a warm white color

temperature was explored. In section 2.4, the maximum efficacy of the system was calculated, considering various laser WPE, and the extraction efficiency was modeled as a function of phosphor plate sidewall angle. Advanced methods for improving the phosphor plate design were simulated and experimentally tested in the form of a wavelength selective reflective coating (section 2.5).

2.1. Color point tuning

In a transmission geometry with a blue laser and a yellow single crystal phosphor, the optical path length of the laser through the phosphor controls the color point. To form a white light output, there is some phosphor thickness for a given geometry and laser power that will place the color point on the Planckian locus. A series of single crystal Ce:YAG phosphors with thicknesses varying from 530 to 1450 μm were fabricated with equilateral triangle shapes and side lengths on the order of 1 mm per side. The phosphors side lengths were well controlled due to the dicing process. The phosphors were mounted within the compact setup with the laser run at a constant current of 1 A to pump each phosphor. Tests were conducted to collect all the light leaving each phosphor and determine the color point of the emitted light integrated over all directions, plotted in Figure 4. Varying the thickness of the phosphor tuned the color point as expected, becoming more yellow with increasing thickness, and an optimal thickness of ~640 μm was found for these laser-phosphor conditions. A one laser, one phosphor system allowed for color points that created a straight line on the CIE color diagram as in Figure 4, such that only cool color temperatures of white light could be reached. In order to

reach more points on the CIE color diagram and a wider range of color temperatures, the laser and phosphor components need to be changed or more components need to be added. Achieving warm white lighting is of interest for many lighting applications. Red light in the form of either a red laser or a red phosphor can shift the color point to allow for a warm white light.

2.2. Warm white: Using a red laser

In the case of adding a red laser, the efficiency of the system will depend on the WPE of the red laser as well as previously considered factors. The WPE of high-efficiency AlInGaP red laser diodes at 638 nm is ~45% [47], similar to that of a high-efficiency blue laser diode. The laser diodes should be separately controlled due to differences in electrical characteristics, providing an additional degree of freedom when controlling the color point of the system. Simulations were conducted to determine the design space for this two-laser system. The optical power of the bluer laser was kept fixed at 1 W. The thickness of the single crystal phosphor was increased from 0.02 to 0.6 mm and the red laser optical power was switched from 0 to 600 mW. All emitted light was collected in the simulation as if using an integrating sphere. Figure 5 presents the CIE diagram of the emission achievable with a system composed of a blue 440 nm laser, a red 640 nm laser, and a Ce:YAG single crystal phosphor. Each component had a dominant color in the CIE diagram and were at the edge of a triangle describing the color theoretically achievable by the system. The side of triangle between the 440 nm laser and the Ce:YAG phosphor described the color achievable with the red laser turned off. On

this line, the phosphor thickness tuned the color point in a similar fashion to what was experimentally shown in Figure 4, although the phosphor crystal geometry and laser power differed in the simulation and experiment. In this system and with the red laser off, a thickness of 0.06 mm allowed the achievement of a white emission close the Planckian locus with a CCT of 6200K and a luminous flux of 215 lm.

Figure 6 presents the details of the luminous flux, efficacy, CRI, and CCT of the two laser plus single crystal phosphor system for different phosphor thickness and red laser power. For a given phosphor thickness, the increase in red laser power increased the luminous flux due to the increase in the light entering the system. The efficacy of the system also increased, however this parameter was largely dependent on the assumed efficiency of the red laser diode. The CRI of the system increased initially with the addition of the red laser diode but did not continue to increase as the laser power was increased more. The addition of a red source, specifically a narrow linewidth red source such as a laser, is consistent with an improved CRI [8,33,48,49]. The CCT decreased with the addition of the red laser diode, which was the initial motivation for the second laser. Increasing the power of the red laser diode allowed warmer color temperatures to be reached. A phosphor thickness of 0.20 mm together with a red laser diode operating around 400 mW showed emission of white light with a CCT of 3000K and a luminous flux above 300 lm.

A practical concern when using a red laser is the color mixing resulting in the combination of the additional laser light with the blue laser-yellow phosphor light. We are proposing herein a design to improve color mixing

in which a red laser is used in conjunction with a single crystal phosphor selectively coated with reflective material. As this design requires the use of two lasers, testing was conducted separately from the compact setup as a proof of concept. A square single crystal phosphor with side length on the order of 1 cm and a thickness of 470 µm was partially coated with a white, reflective TiO_2-based paint. The side of the phosphor facing the lasers was entirely coated other than a central window to allow the laser light to pass into the phosphor. The other side of the phosphor was coated only in the center, opposite where the laser window was left uncoated. Figure 7a and Figure 7b indicate the geometry of the coating on the phosphor plate. The coating used here was not highly reflective but served only as an initial example of the geometry proposed. A red laser (633 nm) and a blue laser (441 nm), both commercially purchased as packaged devices, were directed towards the center opening in the paint on the backside of the phosphor and the light was detected on the opposite side to determine the color point. The selective coating was studied in order to improve color uniformity at the output of the device as well as decreasing the amount of phosphor material necessary. In this design, the laser light travels through the phosphor thickness multiple times, increasing the effective optical path length through the phosphor approximately threefold and therefore decreasing the amount of phosphor necessary to reach the desired color point (Figure 7c). Although the red laser was not being used for conversion, in this design the red laser traveled through the single crystal phosphor in a similar fashion to the blue laser. Additionally, the laser light that survives the passes through the phosphor, including the

red laser light, would be further spread by the multiple bounces in the phosphor plate.

The lasers were individually controlled with the optical powers varied between 0.015 and 0.29 W for the red laser and between 0.085 and 0.486 W for the blue laser. Due to limitations on our measurement setup, this measurement was not conducted in an integrating sphere and the color point was instead measured on light emitted from the topside of the phosphor. A white light with a color temperature of 3000K was obtained at several different blue and red laser powers. This system had the benefit of being able to tune each laser individually to have control over the color point, however integrating both lasers into a package with a small single crystal phosphor was not achievable using commercially available lasers and limited optics. With proper packaging and laser driver design, a multi-laser system could be a path towards warm white laser lighting [33].

2.3. Warm white: Using a red phosphor

Alternatively, a red phosphor may be incorporated into the system as an additional down-conversion source with potentially lower cost and simpler device design. Rather than driving two lasers with different properties, the addition of the red phosphor would not change the operation of the system after fabrication. Although red phosphors are less efficient and less studied quantitatively in lighting systems than the yellow phosphor Ce:YAG, they continue to improve with further research efforts [50,51]. The down-conversion of the blue laser light to red contributes to a higher Stokes shift, reducing efficiency in comparison to the one-phosphor system or the two-laser system with a high efficiency red laser diode.

The choice of red phosphor material has similar considerations to the yellow phosphor material, with the addition of needing to be controllably added to the system in small amounts. This makes the use of a red phosphor powder adhered to the yellow single crystal phosphor an attractive choice. The use of a sol-gel process to adhere the red phosphor powder to the single crystal phosphor can allow for varying amounts of red phosphor to be added to the system. Additionally, the thermal conductivity of the sol-gel can potentially be high enough to allow for appropriate heat transfer, in comparison to other encapsulants such as silicone [40,52]. Ideally, for optimal heat transfer from the red phosphor, the red phosphor particles would be in direct contact with the single crystal surface, with the sol-gel serving as a sticking agent. Red phosphor powder, $CaSiAlN_3:Eu^{2+}$, was suspended in a TiO_2 sol-gel (titanium isopropoxide, ethanol, acetic acid) and drop cast onto a single crystal of Ce:YAG (~1 mm square). The single crystal was baked a 60 °C between drops and then annealed in air at 300 °C for 30 min. This deposition was shown to shift the color of the light towards red when tested in the compact setup, as given by the spectrum in Figure 8. For this warm white method, more iterations are necessary to establish the correct thickness of the single crystal and amount of red phosphor to achieve the desired white point.

In comparison to the two-laser system, every iteration to determine the appropriate amounts of red phosphor necessitates fabricating a new phosphor plate instead of changing the power of the red laser. However, this work demonstrated the ability to introduce red light into a compact setup without complex packaging – something which was not an option for

the two-laser design where a compact setup was not achieved here. For an application in which a single driver was desired or little processing and packaging was available, the two-phosphor system presents an attractive choice. However, when the ability to drive multiple lasers and create more compact packages is not a concern, using two lasers provides a system that can be further tuned after packaging and appropriately simulated, as well as potentially providing a higher CRI and efficacy.

2.4. Single crystal Ce:YAG designs: Improving efficacy

By considering Equation 1, assumptions can be made to estimate the upper limit to efficacy of a laser lighting system. For a cool white system using a given blue wavelength and yellow phosphor, the QY and SS are fixed by the phosphor and the LER is fixed by the white point. The OE and the WPE are then controllable parameters, where the OE is set by the single crystal design and package and the WPE is a function of the laser. Figure 9 presents the simulated efficacy and luminous flux achievable with a blue laser and yellow phosphor system for different laser WPE, with the OE fixed at 90%. This OE value was chosen for the calculations in order to simulate a system with a highly efficient package. As expected, the WPE drastically impacts the performance of the device. Reaching 1000 lm single emitter devices at 160 lm/W, the current state of the art efficiency for high power single die white LEDs [53], will require the OE to be 90% and the WPE to be 50%. As the state of the art blue laser diode becomes more efficient, the efficacy of the system will increase. Equally important is reaching an OE of 90%, which relies on significant package

considerations including the processing of an efficient phosphor plate with high in-coupling of the laser and high extraction efficiency.

Designs for single crystal phosphors can utilize knowledge gained from LED packaging designs as a starting point to further optimize the extraction efficiency and directionality of the output light. Ray tracing simulations are a useful tool for modeling such designs. A parallelepiped phosphor with sidewalls of varying angle was modelled using MCRT with a point light source, set at the center of the parallelepiped, with a power of 1 W. The extracted light was collected and the ratio of the extracted power over the emitted power gave the extraction efficiency while the sidewall angle was changed. This simulation considered the escape of the light from the phosphor to the outside of the single crystal, neglecting weak background absorption of the phosphor single crystal. For straight sides, the extraction efficiency was around 50%, where a portion of the light was trapped within guided modes. Angles above 4° allowed for 100% theoretical extraction efficiency. This result can be applied to the escape of the phosphor light as well as the escape of the laser light from the single crystal. By deviating from a parallelepiped design in any dimension, more light could escape. For the experimental work in this study, in-plane shaping was utilized to improve extraction efficiency, with an equilateral triangular shape picked to conserve material and for ease of fabrication. In-plane triangular shaping serves to increase the extraction by breaking the symmetry in the plane and allowing for more light to escape out of the sidewalls.

Out of plane trapezoidal shaping by angled sidewalls could additionally increase extraction by directing light upwards into the extraction cone. Rather than implementing out of plane shaping experimentally, the extraction could be increased by using roughening of the top surface, a method used in LED packaging techniques [54]. Instead of directing the light into the extraction cone by angled sidewalls, the roughened surface effectively increases the acceptance angle of the escape cone as well as randomizing the reflections to promote multi-pass extraction.

2.5. Wavelength-dependent coating to improve efficacy

Although methods to improve extraction efficiency can be drawn from LED work, for LEDs the phosphor material typically encases the LED where adding the encapsulant improves the out-coupling from the GaN LED. In the case of laser lighting, the laser is outside of the phosphor material. Some sources of loss are depicted in Figure 10(a). One source of loss is due to the reflection of the laser at the surface of the phosphor. Any amount of laser light that gets reflected back by the phosphor surface is lost due to absorption by the laser packaging. Given the index of refraction of the single crystal ($n = 1.82$) [55,56], the percentage of incoming light reflected at normal incidence for a phosphor with an optically smooth interface was calculated to be 8.5%. This loss can be reduced by the addition of an antireflective (AR) coating such as a quarter-wavelength coating tuned for the laser wavelength. While an AR coating would serve to help with the laser in-coupling efficiency, it may also serve to increase the amount of yellow light extracted out of the bottom of the phosphor. In the transmission geometry, yellow phosphor light extracted in the

downwards direction towards the laser would be another source of loss due to absorption by the package.

A coating that is reflective in the yellow range and transmissive in the blue range is therefore desired. As indicated in Figure 10(b), this coating could minimize in-coupling losses as well as losses due to downward reflection of yellow light. Such a coating could take the form of a distributed Bragg reflector (DBR) or a Fabry-Pérot coating (FP), either of which would be designed to have wavelength dependent reflectivity over the visible wavelength range. A DBR with the structure in Figure 11(a) and a FP with the structure in Figure 11(b) are two examples of potential coatings. In these structures, the optical thicknesses of the thinner layers were λ/4 thick. The resonant Ta_2O_5 cavity was λ/2 thick in the FP. The SiO_2 side was in contact with the single crystal for both designs. The choice of dielectric material and periodicity was not unique, as a variety of designs may achieve varying levels of reflectivity.

Transmission matrix simulations indicating the theoretical reflectivity spectra for a representative coating of each type are shown in Figure 12. The target wavelength maximum for the DBR was 570 nm with three periods. The target wavelength minimum for FP resonance was 442 nm to match the experimental wavelength of a laser initially tested. The FP coating in Figure 11(b) was deposited on a polished Ce:YAG single crystal using ion beam deposition (IBD, Veeco NEXUS). Layer thicknesses and refractive indices were calibrated using ellipsometry and the overall FP coating was calibrated by iterating on FP depositions and adjusting layer thicknesses. Using a similar method, the deposition of a DBR coating was

also attempted. Whereas the FP coating could be calibrated to have a minimum at the laser wavelength, the DBR coating was calibrated with respect to the wavelength of maximum reflectance. The fringes and minima were then heavily dependent on precise control of deposition rates and refractive indices, such that a DBR with a minimum at the laser wavelength was difficult to achieve and not reported herein. Normal reflectivity measurements (Filmetrics F20) were measured on reference polished sapphire pieces and on the final FP coated single crystal phosphor from the backside of the phosphor, given in Figure 12. The theoretical minimum reflectivity was 1.2%, whereas the experimentally achieved minimum value was ~3%. In addition, there was significant overlap of the phosphor emission spectrum and the wavelengths of higher reflectivity.

A series of phosphors was then tested with and without the presence of a FP coating, in order to provide an initial demonstration of the coating technology presented. A FP coated phosphor single crystal was diced into triangles (~ 1 mm per side, 800 µm thick) and the diced phosphors were compared to a set of uncoated single crystals (~ 1 mm per side, 850 µm thick), where all phosphors had the same equilateral triangle shape and side length. The marginally thicker phosphor was used as the uncoated sample so that any increase in phosphor extraction provided by the FP coating could be attributed to the coating and not to the thickness difference. Ten tests were conducted in which the laser was tested alone, followed by testing of an uncoated sample, followed by a sample with the FP coating. The compact setup was utilized in each case. For each pair of uncoated and coated samples, the WPE of the laser was experimentally

determined prior to each test by measuring the laser alone in the integrating sphere and taking the ratio of the optical power to the electrical power as the WPE. The WPE was tested before each pair of samples in order to consider laser fluctuations. The average laser WPE measured in this fashion was 2.4%, considerably lower than the best available commercial blue lasers. While these lasers were far from optimal, they served here to evaluate the wavelength selective coating and were not expected to reach the high efficacy values calculated in Figure 9. The relative optical efficiency of the emitter was estimated based on Equation 2, a rearrangement of Equation 1. The QY and SS were 90% and 78%, respectively, for the phosphors used in this work. The QY was experimentally verified (see Experimental) while the SS was calculated given the laser wavelength and the phosphor emission spectrum. Although Equation 2 does not consider that the QY and SS only apply to the light being absorbed and converted by the phosphor, respectively, the relative estimation for optical efficiency should be comparable sample to sample.

$$OE = \frac{Efficacy\left(\frac{lm}{W}\right)}{WPE\,x\,QY\,x\,SS\,x\,LER\left(\frac{lm}{W}\right)} \quad (2)$$

The average efficacy, LER, and OE were all greater in the samples with the FP coating. The average efficacy increased by 22%, from 2.7 lm/W to 3.3 lm/W, with the addition of the FP coating. While the efficacy numbers were lower than desired, this was as expected from the low measured WPE of the laser. For each trial, the sample with the wavelength selective

coating showed a higher efficacy than the sample without the coating. Figure 13(a) compares the OE of each sample over the order of testing the samples, showing that effects from any deviations in the laser power were mitigated. The average relative OE was 45% and 52% for the samples without and with the FP coating, respectively. The improvement in OE with the addition of the FP coating was attributed to better in-coupling of the laser as well as better extraction of the phosphor light. Figure 13(b) shows a comparison in the maximum of the phosphor peak and the maximum of the laser peak. The phosphors with the coating had more phosphor emission for a given laser peak height. This led to the increase in LER with the introduction of the FP coating, as the yellow phosphor light overlaps more with the eye response function than the blue laser light. The average LER without the coating was 364 lm/W and with the FP coating was 385 lm/W. The increase in LER also suggests that the use of a FP coating can allow for less phosphor material to be used in order to achieve the desired white point. The increase in LER with the increase in OE together form the basis for the reported increase in luminous efficacy in the emitter.

3. Conclusion

We have demonstrated variations of laser based white lighting systems using a phosphor single crystal in a transmission geometry. A compact emitter design was presented and ways to optimize optical efficiency, decrease the amount of phosphor material, and tune the color temperature were discussed. Adding a red laser to the system achieved a white light of ~3000K. Simulations with two lasers showed the ability to

retain good efficiency, although the system would require custom laser packaging and additional laser driver electronics. The addition of a red phosphor powder also provided a red light for warm white light and allowed for a design with minimal packaging requirements but was less optimal for efficiency. A wavelength selective reflective coating improved efficacy 22% by increasing in-coupling efficiency and decreasing phosphor light emitted backwards while also decreasing the amount of phosphor material necessary. Ultimately, widespread adoption of laser lighting will necessitate research on high collection efficiency luminaires as well as commercially available lasers with wall-plug efficiency of at least 50%. However, the methods described herein may be applied to future laser lighting systems where a transmission geometry would be more viable than a reflection geometry, including broad area illumination using fiber systems.

4. Experimental Section

Simulations

Optical simulations were carried out using the commercial software LightTools™, based on the Monte Carlo Ray Tracing (MCRT) method. Based on the law of geometrical optics, MCRT allows modeling of both the optical package and of the phosphor plate. The blue and red laser diode spectra, the emission, absorption, and excitation spectra as well as the QY of the phosphor used in this study were experimentally measured and implemented in the simulation. To test our modeling, a Ce:YAG single crystal was shaped into a 5x1x0.2 cm rectangular cuboid and excited with a 440 nm blue laser diode. The spectral density function (SDF) of the

system was measured in an integrating sphere. The system was then simulated with the MCRT method. Figure 14 presents the simulated and measured SDF for the blue laser and single crystal phosphor system, where there was excellent agreement between the simulation and the experiment. In the case of single crystal phosphors, the optical modeling by ray tracing does not increase in complexity greatly with the addition of the phosphor, in the sense that simulations of single crystal phosphors are well achieved and very reproducible. In comparison, simulations on powder and ceramic phosphor compounds have to be adjusted manually to fit the experimental data [57]. These simulations assume that the particles are spherical, are mono disperse in size and position [58], and that Mie theory can be applied [57,59,60]. In particular, the mean free path is a complex quantity to measure and difficult to implement in a simulation [61]. For these reasons, single crystal phosphors may be finely tuned into optical systems more exactly through precise modeling.

Phosphor plate fabrication and testing

Ce:YAG single crystal yellow phosphors were used in this work, with 0.2% to 0.3% Ce content (atomic percent). The phosphors were synthesized by Saint-Gobain and found to have a QY of 90%, based on measurements conducted in an integrating sphere on a phosphor piece with polished and parallel sides. The SS was calculated to be 78%, considering the energy difference between the laser wavelength and phosphor emission spectrum. The crystals were polished and had various sizes and shapes or were cut to the desired shape and size. In order to control the sample thickness, larger pieces of single crystal were cut into slices using a wire

saw. Chemical mechanical polishing was conducted to further thin and polish the phosphor plates. Roughness was measured via atomic force microscopy (AFM). Rough surfaces were prepared using a diamond polishing pad for as received or polished facets, with as-cut sample facets being sufficiently rough. To obtain small pieces of single crystals, a dicing saw was used with the ability to dice phosphors into squares or triangles on the order of 1 mm per side. An example of a diced Ce:YAG single crystal is shown in Figure 15, along with atomic force micrographs of the crystal before and after chemical mechanical polishing. The RMS roughness before polishing was 421 nm and was reduced to 9 nm after polishing. As cut and prior to polishing, the surface was sufficiently rough to improve topside light extraction from the phosphor. After polishing, the backside surface was smooth to allow for coupling of the laser into the phosphor without light scattering. This smooth surface was also necessary for subsequent layer deposition described later.

Testing of phosphors was conducted using commercial laser diodes packaged in TO9 cans with emission wavelengths between 440 nm and 445 nm. The TO9 cans were mounted in machined copper heat sinks such that the base of the TO9 can sits in the heat sink and the top portion extends above the heat sink. Small phosphors were mounted in machined copper mounts with prongs holding the single crystal directly above the output of the laser with the roughened surface of the phosphors pointing away from the laser and the smooth side facing the laser. The copper phosphor mounts were machined for both triangular and square phosphors, and the style of the mount was modified somewhat for various

experiments. The copper phosphor mount was in contact with the copper laser heat sink and was secured to the TO9 cans using set screws to adjust the phosphor position in front of the laser beam. A labeled image of the compact emitter is shown in Figure 3. The setup was tested to check for potential quenching of the phosphor due to high temperatures, and it was noted that sufficient contact between the prongs of the holder and the phosphor itself was required to prevent quenching. All measurements were conducted within a regime where phosphor quenching effects did not occur.

Measurements were conducted in an integrating sphere coupled to a spectrometer unless otherwise stated. The laser diodes were run under continuous-wave operation. Various laser diodes were used across different experiments as the laser diodes were seen to degrade across multiple tests. Measurements were corrected for every laser used. A neutral density filter was used and results include approximate corrections for the filter.

Acknowledgements

This work was supported in part by the Solid State Lighting and Energy Electronics Center (SSLEEC) at the University of California, Santa Barbara. The information, data, or work presented herein was funded in part by the Advanced Research Projects Agency-Energy (ARPA-E), U.S. Department of Energy, (DE-AR0000671). The views and opinions of authors expressed herein do not necessarily state or reflect those of the United States Government or any agency thereof. Some phosphor materials were obtained through a collaboration with Saint-Gobain. A portion of this work was performed in the UCSB Nanofabrication Facility, an open access laboratory. A portion of this work made use of MRL Shared Experimental Facilities, MRSEC Program, NSF (DMR 1720256). A portion of this work made use of MRL Central Facilities, MRSEC Program, NSF, (DMR 1121053).

Received: ((will be filled in by the editorial staff))
Revised: ((will be filled in by the editorial staff))
Published online: ((will be filled in by the editorial staff))

References

1. M. Yamada and D. Chwastyk, *Adoption of Light-Emitting Diodes in Common Lighting Applications* (2013).
2. J. Penning, S. Schober, K. Stober, and M. Yamada, *Adoption of Light-Emitting Diodes in Common Lighting Applications* (2017).
3. M. Yamada, J. Penning, S. Schober, K. Lee, and C. Elliott, *Energy Savings Forecast of Solid-State Lighting in General Illumination Applications* (2019).
4. M. H. Keuper, G. Harbers, and S. Paolini, "26.1: RGB LED Illuminator for Pocket-Sized Projectors," Soc. Inf. Disp. **35**, 943–945 (2004).
5. P. Pust, P. J. Schmidt, and W. Schnick, "A revolution in lighting," Nat. Mater. **14**, 454–458 (2015).
6. C. Weisbuch, M. Piccardo, L. Martinelli, J. Iveland, J. Peretti, and J. S. Speck, "The efficiency challenge of nitride light-emitting diodes for lighting," Phys. Status Solidi Appl. Mater. Sci. **212**, 899–913 (2015).
7. M. R. Krames, O. B. Shchekin, R. Mueller-Mach, G. O. Mueller, L. Zhou, G. Harbers, and M. G. Craford, "Status and future of high-power light-emitting diodes for solid-state lighting," J. Disp. Technol. **3**, 160–175 (2007).
8. P. Pust, V. Weiler, C. Hecht, A. Tücks, A. S. Wochnik, A. K. Henß, D. Wiechert, C. Scheu, P. J. Schmidt, and W. Schnick, "Narrow-band red-emitting $Sr[LiAl_3N_4]:Eu^{2+}$ as a next-generation LED-phosphor

material," Nat. Mater. **13**, 891–896 (2014).

9. Y. H. Kim, N. S. M. Viswanath, S. Unithrattil, H. J. Kim, and W. Bin Im, "Review—Phosphor Plates for High-Power LED Applications: Challenges and Opportunities toward Perfect Lighting," ECS J. Solid State Sci. Technol. **7**, R3134–R3147 (2018).
10. C. Cozzan, G. Lheureux, N. O 'Dea, E. E. Levin, J. Graser, T. D. Sparks, S. Nakamura, S. P. Denbaars, C. Weisbuch, and R. Seshadri, "Stable, Heat-Conducting Phosphor Composites for High-Power Laser Lighting," ACS Appl. Mater. Interfaces **10**, 5673–5681 (2018).
11. K. G. Kedawat, P. Kundu, R. Srivastava, J. K. Jain, H. C. Kandpal, and B. K. Gupta, "High Power Laser-Driven Ce^{3+}-Doped Yttrium Aluminum Garnet Phosphor Incorporated Sapphire Disc for Outstanding White Light Conversion Efficiency," Phys. Status Solidi Appl. Mater. Sci. **216**, 1900110 (2019).
12. E. A. Salazar-Valenzuela, J. Alvarado-Rivera, C. Chapa, and M. E. Álvarez-Ramos, "Recycled Glass and YAG:Ce^{3+} Nanoparticles Phosphor-in-Glass for WLEDs Applications," Phys. Status Solidi 2000226 (2020).
13. H. König, M. Ali, W. Bergbauer, J. Brückner, G. Bruederl, C. Eichler, S. Gerhard, U. Heine, A. Lell, L. Nähle, M. Peter, J. Ristic, G. Rossbach, A. Somers, B. Stojetz, S. Tautz, J. Wagner, T. Wurm, U. Strauss, M. Baumann, A. Balck, and V. Krause, "Visible GaN laser diodes: from lowest thresholds to highest power levels," Proc SPIE **10939**, 109390C (2019).
14. J. J. Wierer and J. Y. Tsao, "Advantages of III-nitride laser diodes in

solid-state lighting," Phys. Status Solidi Appl. Mater. Sci. **212**, 980–985 (2015).

15. K. A. Denault, M. Cantore, S. Nakamura, S. P. Denbaars, and R. Seshadri, "Efficient and stable laser-driven white lighting," AIP Adv. **3**, 072107 (2013).
16. C. Basu, M. Meinhardt-Wollweber, and B. Roth, "Lighting with laser diodes," Adv. Opt. Technol. **2**, 313–321 (2013).
17. B. Berk, "The Headlight of the Future Is a Laser," Bloomberg (2019).
18. C. Lee, C. Shen, H. M. Oubei, M. Cantore, B. Janjua, T. K. Ng, R. M. Farrell, M. M. El-Desouki, J. S. Speck, S. Nakamura, B. S. Ooi, and S. P. DenBaars, "2 Gbit/s data transmission from an unfiltered laser-based phosphor-converted white lighting communication system," Opt. Express **23**, 29779 (2015).
19. C. Lee, C. Zhang, M. Cantore, R. M. Farrell, S. H. Oh, T. Margalith, J. S. Speck, S. Nakamura, J. E. Bowers, and S. P. DenBaars, "4 Gbps direct modulation of 450 nm GaN laser for high-speed visible light communication," Opt. Express **23**, 16232–16237 (2015).
20. F. Zafar, M. Bakaul, and R. Parthiban, "Laser-Diode-Based Visible Light Communication: Toward Gigabit Class Communication," IEEE Commun. Mag. **55**, 144–151 (2017).
21. A. Ooi, A. Wong, T. Khee Ng, C. Marondedze, C. Gehring, and B. S. Ooi, "Growth and development of Arabidopsis thaliana under singlewavelength red and blue laser light," Sci. Rep. **6**, 33885 (2016).
22. J. D. Unsworth, "METHOD FOR CREATING SIDE FIRING OR LEAKY OPTICAL FIBERS," U.S. patent US 6,606,431 B2 (2003).

23. K. W. Bennett, E. J. Fewkes, S. L. Logunov, and V. Tyagi, "Light diffusing optical fiber bundles, illumination systems including light diffusing optical fiber bundles, and methods of affixing light diffusing optical fiber bundles to polymer optical fibers," U.S. patent US008967845B2 (2015).

24. L. Y. Kuritzky, C. Weisbuch, and J. S. Speck, "Prospects for 100% wall-plug efficient III-nitride LEDs," Opt. Express **26**, 16600 (2018).

25. M. G. Peters, D. B. Young, F. H. Peters, B. Thibeault, J. W. Scott, S. W. Corzine, R. W. Herrick, and L. A. Coldren, "High wall-plug efficiency temperature-insensitive vertical-cavity surface-emitting lasers with low-barrier p-type mirrors," Proc. SPIE Vertical-Cavity Surface-Emitting Laser Arrays **2147**, 2–11 (1994).

26. G. Blasse and A. Bril, "Investigation of Some Ce3+-Activated Phosphors," J. Chem. Phys. **12**, 5139–5145 (1967).

27. N. C. George, K. A. Denault, and R. Seshadri, "Phosphors for Solid-State White Lighting," Annu. Rev. Mater. Res. **43**, 481–501 (2013).

28. S. Arjoca, E. G. Víllora, D. Inomata, K. Aoki, Y. Sugahara, and K. Shimamura, "Ce:$(Y_{1-x}Lu_x)_3$ Al_5O_{12} single-crystal phosphor plates for high-brightness white LEDs/LDs with high-color rendering (Ra > 90) and temperature stability," Mater. Res. Express **1**, 25041 (2014).

29. C. Oleari, ed., "Chromaticity Diagram from Newton to the CIE 1931 Standard System," in *Standard Colorimetry* (John Wiley & Sons, Ltd, 2015), pp. 237–251.

30. J. D. T. Kruschwitz, "1931 CIE Chromaticity Diagram," *in Field Guide to Colorimetry and Fundamental Color Modeling* (SPIE, 2018), p. 18.

31. C. S. McCamy, "Correlated color temperature as an explicit function of chromaticity coordinates," Color Res. Appl. **17**, 142–144 (1992).

32. N. T. Tran and F. G. Shi, "Studies of phosphor concentration and thickness for phosphor-based white light-emitting-diodes," J. Light. Technol. **26**, 3556–3559 (2008).

33. A. Neumann, J. J. Wierer, W. Davis, Y. Ohno, S. R. J. Brueck, and J. Y. Tsao, "Four-color laser white illuminant demonstrating high color-rendering quality," Opt. Express **19**, A982–A990 (2011).

34. T. Erdem, S. Nizamoglu, X. W. Sun, and H. V. Demir, "A photometric investigation of ultra-efficient LEDs with high color rendering index and high luminous efficacy employing nanocrystal quantum dot luminophores," Opt. Express **18**, 340–347 (2010).

35. G. He and H. Yan, "Optimal spectra of the phosphor-coated white LEDs with excellent color rendering property and high luminous efficacy of radiation," Opt. Express **19**, 2519–2529 (2011).

36. A. Latynina, M. Watanabe, D. Inomata, K. Aoki, Y. Sugahara, E. García Víllora, and K. Shimamura, "Properties of Czochralski grown Ce,Gd:$Y_3Al_5O_{12}$ single crystal for white light-emitting diode," J. Alloys Compd. **553**, 89–92 (2013).

37. N. Narendran, Y. Gu, J. P. Freyssinier, H. Yu, and L. Deng, "Solid-state lighting: Failure analysis of white LEDs," J. Cryst. Growth **268**, 449–456 (2004).

38. N. M. Rada and G. E. Triplett, "Thermal and spectral analysis of self-heating effects in high-power LEDs," Solid. State. Electron. **54**, 378–381 (2010).

39. M. Dal Lago, M. Meneghini, N. Trivellin, G. Mura, M. Vanzi, G. Meneghesso, and E. Zanoni, "Phosphors for LED-based light sources: Thermal properties and reliability issues," Microelectron. Reliab. **52**, 2164–2167 (2012).

40. C. Cozzan, M. J. Brady, N. O 'Dea, E. E. Levin, S. Nakamura, S. P. Denbaars, and R. Seshadri, "Monolithic translucent $BaMgAl_{10}O_{17}:Eu^{2+}$ phosphors for laser-driven solid state lighting," AIP Adv. **6**, 105005 (2016).

41. S. Arjoca, D. Inomata, Y. Matsushita, and K. Shimamura, "Growth and optical properties of $(Y_{1-x}Gd_x)_3Al_5O_{12}$:Ce single crystal phosphors for high-brightness neutral white LEDs and LDs," CrystEngComm **18**, 4799–4806 (2016).

42. S. Li, A. Qiangqiang Zhu, D. Tang, G. Ouyang, L. Cao, N. Hirosaki, T. Nishimura, Z. Huang, and R.-J. Xie, "Al_2O_3-YAG:Ce composite phosphor ceramic: a thermally robust and efficient color converter for solid state laser lighting," J. Mater. Chem. C **4**, 8648–8654 (2016).

43. M. Raukas, J. Kelso, Y. Zheng, K. Bergenek, D. Eisert, A. Linkov, and F. Jermann, "Ceramic Phosphors for Light Conversion in LEDs," ECS J. Solid State Sci. Technol. **2**, R3168–R3176 (2013).

44. R. MUROTA, T. KOBAYASHI, and Y. MITA, "Solid State Light Source Fabricated with YAG:Ce Single Crystal," Jpn. J. Appl. Phys. **41**, L887 (2002).

45. M. Cantore, N. Pfaff, R. M. Farrell, J. S. Speck, S. Nakamura, and S. P. DenBaars, "High luminous flux from single crystal phosphor-converted laser-based white lighting system," Opt. Express **24**,

A215–A221 (2016).

46. V. Bachmann, C. Ronda, and A. Meijerink, "Temperature quenching of yellow Ce^{3+} luminescence in YAG:Ce," Chem. Mater. **21**, 2077–2084 (2009).

47. M. Hagimoto, S. Miyamoto, Y. Kimura, H. Fukai, M. Hashizume, and S. Kawanaka, "USHIO 3.5W red laser diode for projector light source," Proc SPIE **10939**, 109391I (2019).48. J. H. Oh, H. Kang, Y. J. Eo, H. K. Park, and Y. R. Do, "Synthesis of narrow-band red-emitting $K_2SiF_6:Mn^{4+}$ phosphors for a deep red monochromatic LED and ultrahigh color quality warm-white LEDs," J. Mater. Chem. C **3**, 607–615 (2015).

49. C. Liao, R. Cao, Z. Ma, Y. Li, G. Dong, K. N. Sharafudeen, and J. Qiu, "Synthesis of $K_2SiF_6:Mn^{4+}$ Phosphor from SiO2 Powders via Redox Reaction in HF/KMnO4 Solution and Their Application in Warm-White LED - Liao - 2013 - Journal of the American Ceramic Society - Wiley Online Library," J. Am. Ceram. Soc. **96**, 3552–3556 (2013).

50. Z. Ma, H. Cao, X. Sun, C. Yang, X. Xi, J. Li, S. Lin, and L. Zhao, "Failure Mechanism of Phosphors in GaN-Based White LEDs," Phys. Status Solidi Appl. Mater. Sci. **216**, 1800335 (2019).

51. B. Wang, S. Yao, and W. Li, "Molten-Salt-Assisted Synthesis of $Na_3Bi(PO_4)_2:Eu^{3+}$ Nanoparticles with Strong Red Emission," Phys. Status Solidi Appl. Mater. Sci. **216**, 1800981 (2019).

52. T. Coquil, C. Reitz, T. Brezesinski, E. J. Nemanick, S. H. Tolbert, and L. Pilon, "Thermal Conductivity of Ordered Mesoporous Titania Films Made from Nanocrystalline Building Blocks and Sol-Gel Reagents," J.

Phys. Chem. C **114**, 12451–12458 (2010).

53. DOE BTO SSL Program, *2018 Solid-State Lighting R&D Opportunities* (2019).

54. C. L. Keraly, L. Kuritzky, M. Cochet, and C. Weisbuch, "Light Extraction Efficiency Part A. Ray Tracing for Light Extraction Efficiency (LEE) Modeling in Nitride LEDs," in *III-Nitride Based Light Emitting Diodes and Applications*, T.-Y. Seong, J. Han, H. Amano, and H. Morkoc, eds. (Springer Netherlands, 2013), pp. 231–269.

55. M. Moszyński, T. Ludziejewski, D. Wolski, W. Klamra, and L. O. Norlin, "Properties of the YAG:Ce scintillator," Nucl. Inst. Methods Phys. Res. A **345**, 461–467 (1994).

56. Saint-Gobain, *YAG (Ce) Yttrium Aluminum Garnet Scintillation Material* (2016), Vol. Data Sheet.

57. S.-W. Jeon, J. H. Noh, K. H. Kim, W. H. Kim, C. Yun, S. Bin Song, and J. P. Kim, "Improvement of phosphor modeling based on the absorption of Stokes shifted light by a phosphor," Opt. Express **22**, A1237–A1242 (2014).

58. C. Sommer, F. Reil, J. R. Krenn, P. Hartmann, P. Pachler, S. Tasch, and F. P. Wenzl, "The impact of inhomogeneities in the phosphor distribution on the device performance of phosphor-converted high-power white LED light sources," J. Light. Technol. **28**, 3226–3232 (2010).

59. Z. Liu, S. Liu, K. Wang, and X. Luo, "Measurement and numerical studies of optical properties of YAG:Ce phosphor for white light-emitting diode packaging," Appl. Opt. **49**, 247–257 (2010).

60. D.-H. Lee, J.-Y. Joo, and S.-K. Lee, "Modeling of reflection-type laser-driven white lighting considering phosphor particles and surface topography," Opt. Express **23**, 18872–18887 (2015).

61. V. Y. F. Leung, A. Lagendijk, T. W. Tukker, A. P. Mosk, W. L. IJzerman, and W. L. Vos, "Interplay between multiple scattering, emission, and absorption of light in the phosphor of a white light-emitting diode," Opt. Express **22**, 8190–8204 (2014).

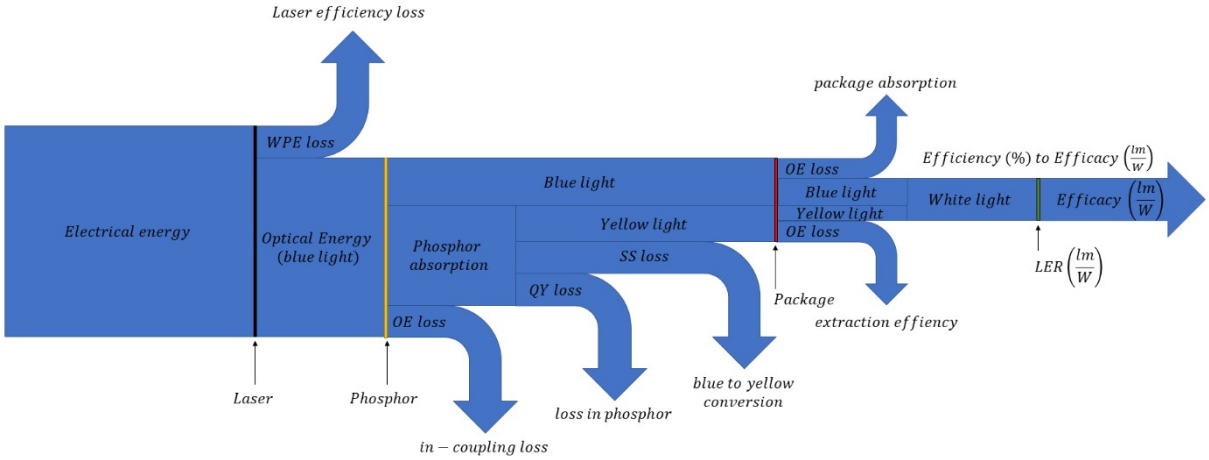

Figure 1. Flow of energy through a generalized blue laser plus yellow phosphor system with components such as the laser, phosphor, and package indicated along with important sources of loss.

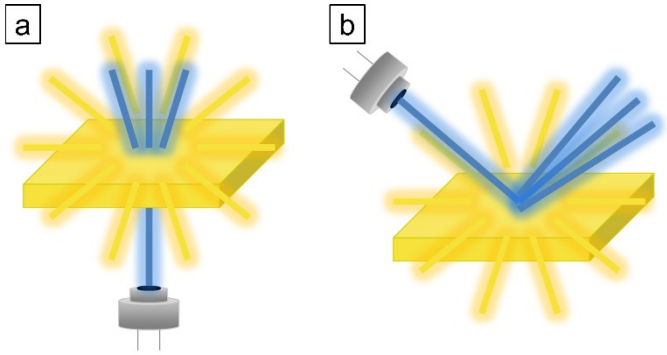

Figure 2. Two main laser/phosphor geometries: (a) transmission and (b) reflection.

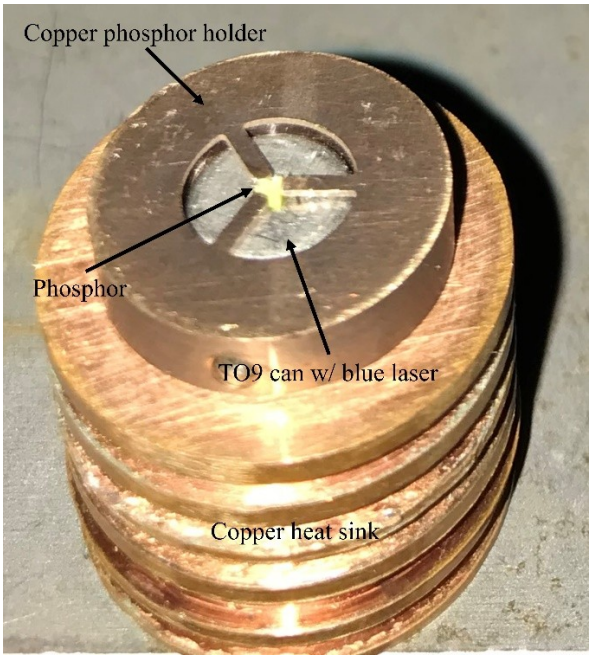

Figure 3. Labeled photograph of compact laser lighting emitter in a transmission geometry with a mounted triangular single crystal phosphor.

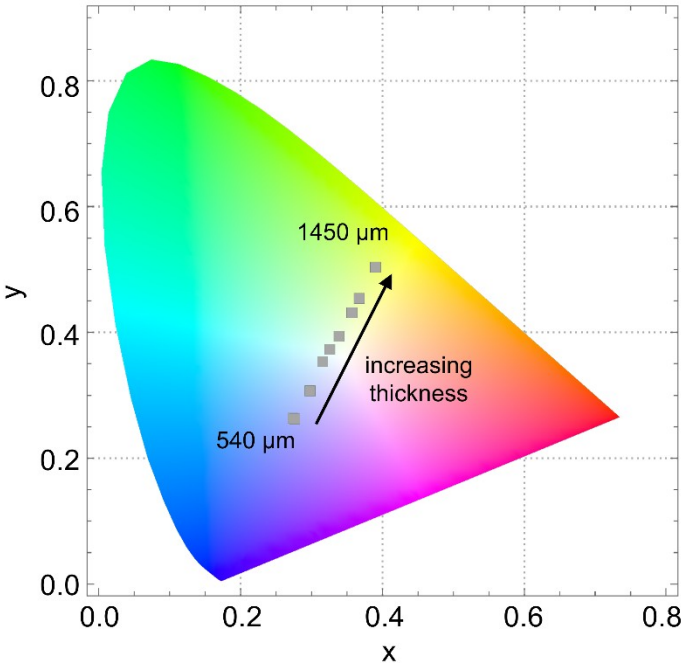

Figure 4. CIE color diagram with points plotted for laser-phosphor emitter with triangular single crystal Ce:YAG phosphors of varying thicknesses.

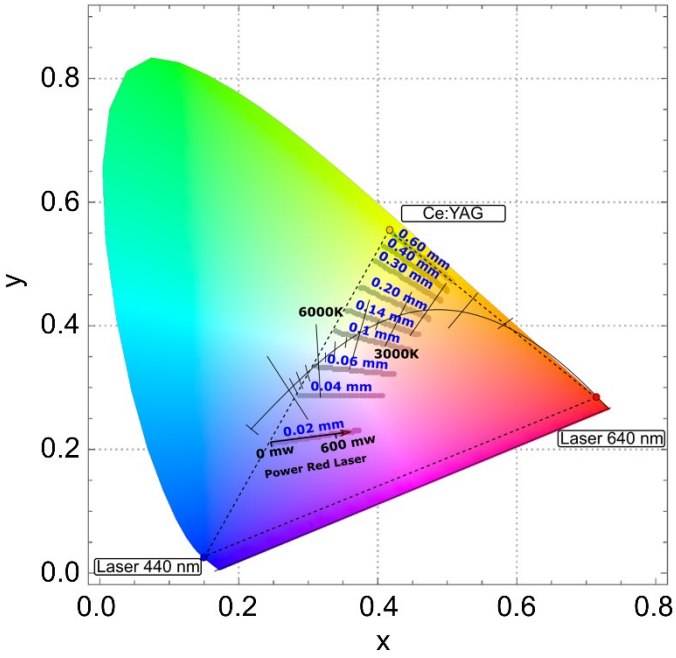

Figure 5. CIE Diagram for a 1 W 440 nm laser, Ce:YAG single crystal phosphor, and 640 nm laser system. The triangle, with corners that are the dominant wavelengths of the three parts, describes the color range achievable. Different phosphor thicknesses were reported (in blue). The blue laser power was kept fixed at 1 W and the power of the red laser diode ranged from 0 to 600 mW.

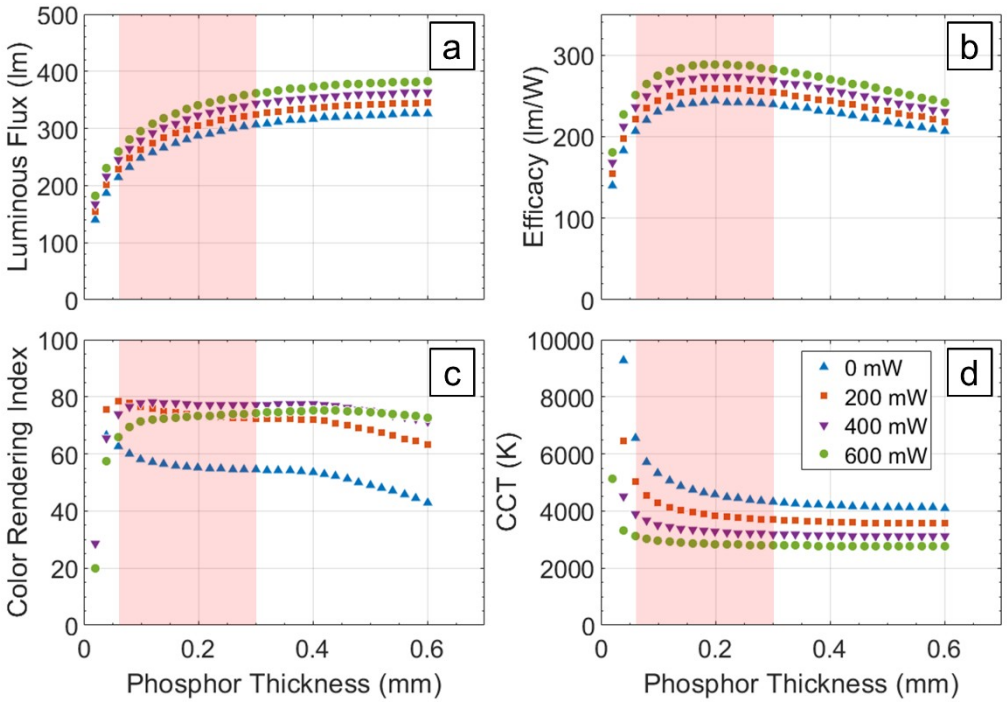

Figure 6. (a) Luminous flux, (b) efficacy, (c) color rendering index (CRI), and (d) correlated color temperature (CCT) of the 1W 440 nm laser + Ce:YAG single crystal phosphor + 640 nm laser system as a function of phosphor thickness for different red laser powers. The shaded regions show the range of single crystal phosphor thicknesses where the emission falls close enough to the Planckian locus to be considered white light.

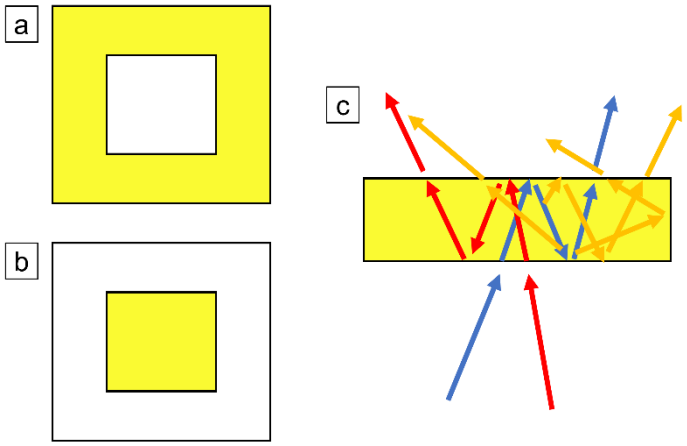

Figure 7. Schematic of two-laser experimental setup with partially coated phosphor plate shown from (a) the topside and (b) the backside; (c) simplified depiction of light inside and escaping the phosphor plate due to reflections at the coated phosphor surfaces with indications of multiple bounces through the phosphor.

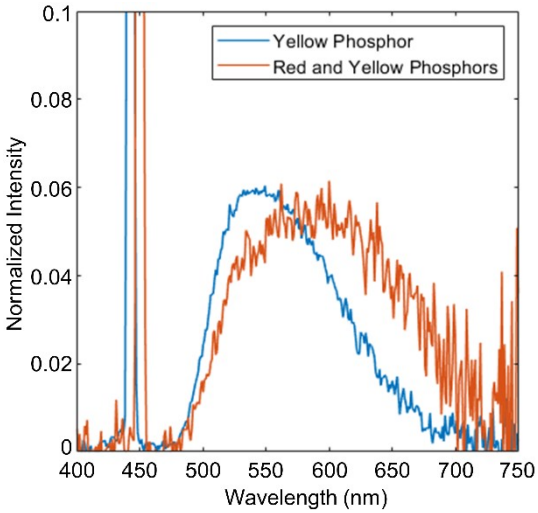

Figure 8. Normalized emission spectra from two laser-phosphor systems, one with single crystal Ce:YAG and one with single crystal Ce:YAG plus red phosphor, $CaSiAlN_3:Eu^{2+}$. Laser peak maxima were normalized to 1 for both spectra.

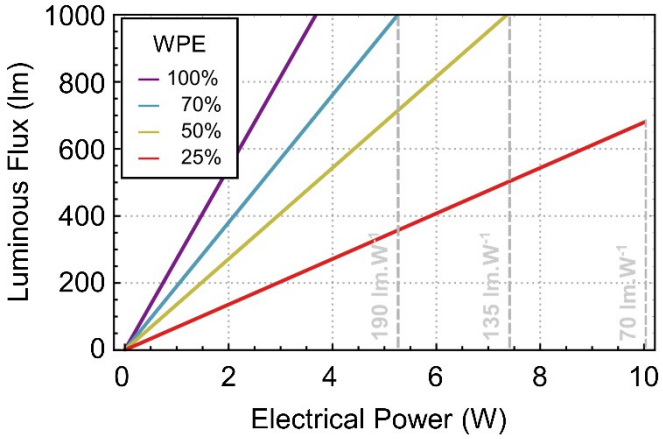

Figure 9. Simulated luminous flux and efficacy achievable with a blue laser + single crystal phosphor system at different electrical power for several laser WPE with the other sources of losses kept constant.

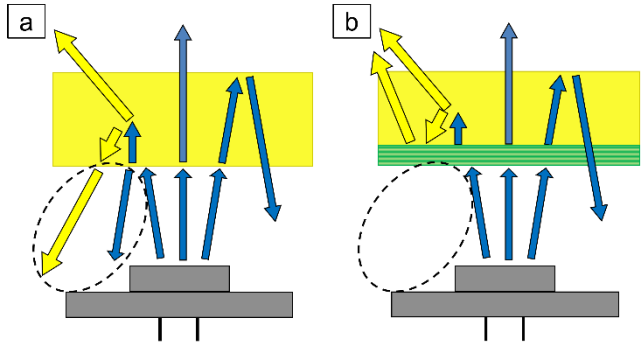

Figure 10. Optical losses in laser-single crystal phosphor emitter (a) without any coating and (b) with a wavelength selective reflective coating represented as alternating green stripes. Sources of losses enclosed in the dashed area in (a) are minimized with the addition of the coating in (b).

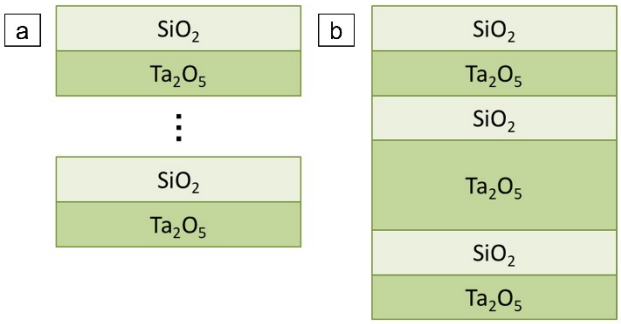

Figure 11. Structures for wavelength-selective reflective coating showing (a) a distributed Bragg reflector (DBR) with λ/4 thick layers and a variable number of periods and (b) a Fabry-Pérot (FP) structure with one layer being λ/2 thick and the rest being λ/4 thick. For the DBR structure, λ is the maximum reflectivity and for the FP structure, λ is the minimum reflectivity.

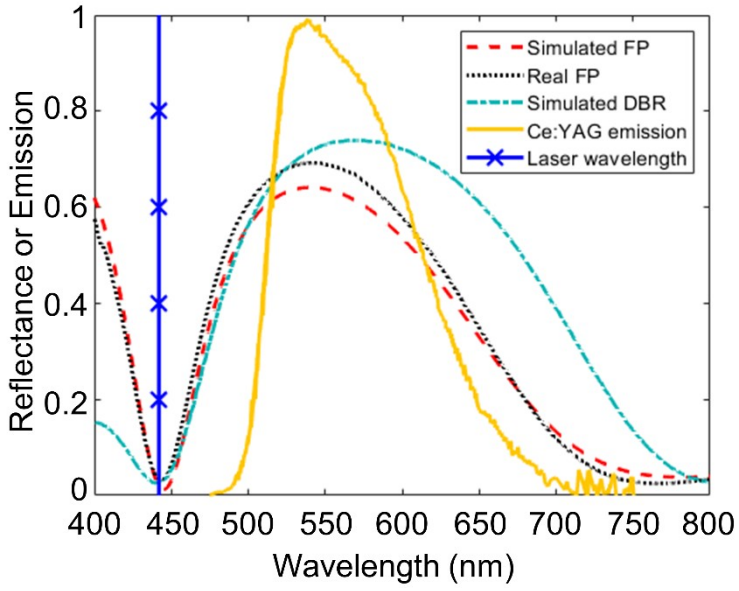

Figure 12. Transmission matrix simulations for wavelength-selective coatings indicating laser wavelength (442 nm), Ce:YAG phosphor emission, simulated normal reflectivity for a distributed Bragg reflector (DBR, 3-period centered at 570 nm), simulated normal reflectivity for the Fabry-Pérot (FP) structure, and experimental reflectivity for the FP.

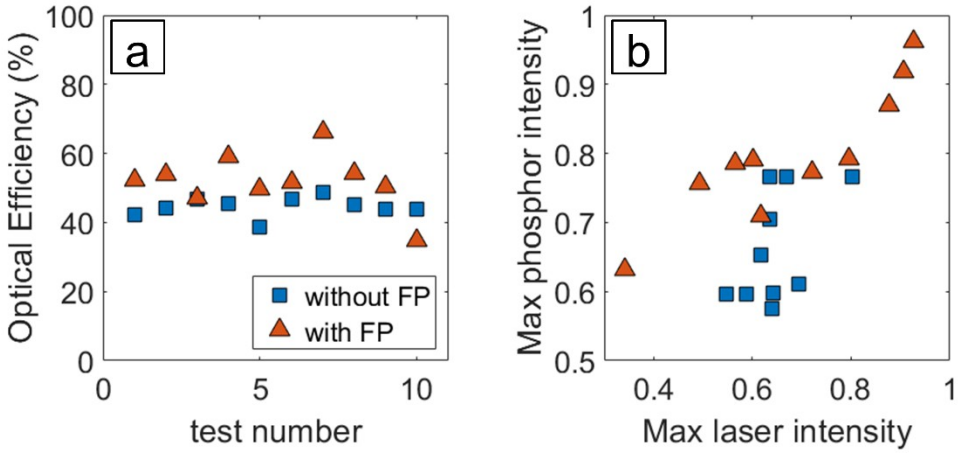

Figure 13. Comparisons between single crystal Ce:YAG phosphors without and with Fabry-Pérot coatings indicating (a) the OE as a function of test number and (b) the maximum phosphor intensity versus the maximum laser intensity.

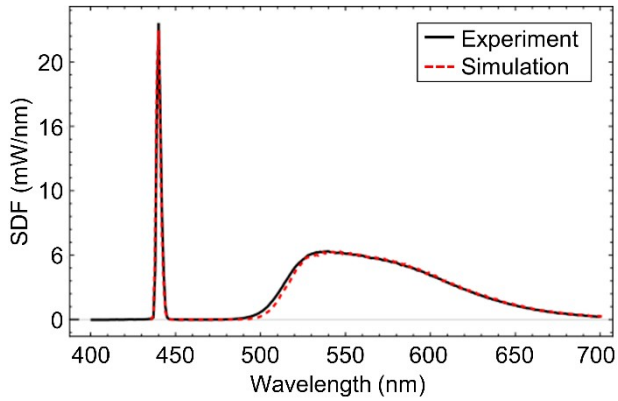

Figure 14. Measured and simulated spectral density function (SDF) of a blue laser diode and a single crystal Ce:YAG phosphor. Single crystal: sample thickness 2 mm, absorption 12 cm^{-1}, laser power 3.5 W.

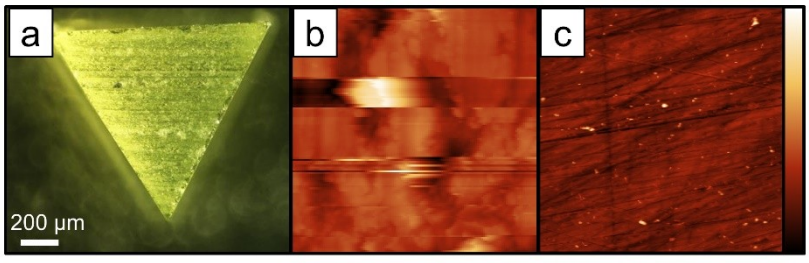

Figure 15. Ce:YAG phosphor single crystal (a) optical microscope image showing triangular shaped phosphor crystal. Atomic force micrographs of Ce:YAG phosphor (b) before chemical mechanical polishing with scale 0 to 3.75 µm and (c) after chemical mechanical polishing with scale 0 to 172 nm. AFM scale designated at right.

The table of contents entry should be 50–60 words long and should be written in the present tense and impersonal style (i.e., avoid we). The text should be different from the abstract text.

Solid-state lighting

Caroline E. Reilly, Guillaume Lheureux, Clayton Cozzan, Emet Zeitz, Tal Margalith, Shuji Nakamura, Ram Seshadri, Claude Weisbuch, and Steven P. DenBaars*

Transmission geometry laser lighting with a compact emitter

A compact emitter for a laser lighting system was created using a commercial nitride laser diode, a small single crystal phosphor, and in-house machined parts. Variations to improve color and efficiency were considered via experiment and simulation, including the addition of a red laser, a red phosphor, or a wavelength-selective coating.